

Universal relation between doping content and normal-state resistance in gate voltage tuned ultrathin $\text{Bi}_2\text{Sr}_2\text{CaCu}_2\text{O}_{8+x}$ flakes

Teng Wang,^{1,2,3} Aobo Yu,^{1,2,4} Yixin Liu,^{1,2,4} Genda Gu,⁵ Wei Peng,^{1,2,4} Zengfeng Di,^{1,4} Da Jiang,^{1,6,*} and Gang Mu^{1,2,4,†}

¹State Key Laboratory of Functional Materials for Informatics, Shanghai Institute of Microsystem and Information Technology, Chinese Academy of Sciences, Shanghai 200050, China

²CAS Center for Excellence in Superconducting Electronics, Shanghai 200050, China

³School of Physical Science and Technology, ShanghaiTech University, Shanghai 201210, China

⁴University of Chinese Academy of Sciences, Beijing 100049, China

⁵Condensed Matter Physics and Materials Science Department, Brookhaven National Laboratory, Upton, New York 11973, USA

⁶Institute for Frontiers and Interdisciplinary Sciences, Zhejiang University of Technology, Hangzhou 310014, China



(Received 9 December 2021; revised 2 August 2022; accepted 29 August 2022; published 14 September 2022)

Gate voltage tunable ultrathin high- T_c cuprates supply a unique platform to investigate the electronic phase diagram and superconductor-insulator transition. One of the challenges in this field is the precise determination of the doping content in the underdoped nonsuperconducting region. Here we report the discovery of a universal relation between the doping content p and the normal-state resistance at a fixed temperature $R(T_f)$, $p = \alpha + \beta \ln[1/R(T_f)]$, in the ultrathin $\text{Bi}_2\text{Sr}_2\text{CaCu}_2\text{O}_{8+x}$ flakes. The in-depth analysis shows that the evolution of carrier scattering probability with doping content and the change of effective mass caused by superconductor-insulator transition are two key factors leading to this logarithmic relation. Based on our finding, the more precise electronic phase diagram can be established. In addition, the superconductor-insulator transition is verified to be a quantum phase transition using a finite size scaling analysis. The scaling exponent $z\nu$ is found to have a close correlation with the disorder levels. The present result provides an important foundation to investigate the fascinating electronic states in the ultra-thin cuprates.

DOI: [10.1103/PhysRevB.106.104509](https://doi.org/10.1103/PhysRevB.106.104509)

I. INTRODUCTION

High- T_c superconductors and low-dimensional materials are two significant platforms to investigate the exotic quantum phenomena. The combination of these two platforms could bring more novel physics. For example, although the electronic phase diagram and superconductor-insulator transition (SIT) have been studied intensively in the bulk sample of high- T_c superconductors [1–7], the ultrathin materials can supply a unique platform to investigate these phenomena by using the electrostatic technique [8–14] which can modulate the carrier density in the order of magnitude of 10^{14} cm^{-2} . This technique has already been adopted in the investigations of the ultra-thin transition metal disulfide superconductors [15–17]. An obvious advantage of this technique is that the experiments can be carried out on one sample, which eliminates many other uncontrollable factors induced by the variation of the samples.

A prerequisite, which is also the main challenge, for this technique is the precise determination of the doping content p in the underdoped nonsuperconducting (non-SC) region. Previously, in most cases, a rather simple relation based on the Drude model, $p = S/R(T_f)$, where S is a constant and $R(T_f)$ is the resistance at a fixed temperature T_f in the normal

state, was adopted [8,9,13,18]. In this treatment, it is assumed that both the relaxation time τ and effective mass m^* are constants during the tuning process. This relation works well in ultra-thin films of $\text{YBa}_2\text{Cu}_3\text{O}_{7-x}$ (YBCO) [9] and flakes of $\text{Bi}_2\text{Sr}_2\text{CaCu}_2\text{O}_{8+x}$ (Bi-2212) [13] with the thickness of 40 nm. In the ultra-thin Bi-2212 system with the thickness of several unit cells, however, the doping content could not be derived accurately by using this relation [12,14], indicating the failure of the simple hypothesis in this system. Although some efforts have been made [14], a reliable and universal route to solve this problem is still lacking up to now. Moreover, the underlying mechanism for the violation of the simple relation has not yet been clarified.

On the other hand, the phase transition between the ground states, which is accompanied by quantum rather than thermal fluctuations, is called the quantum transition [19]. The SIT is typically driven by disorder, magnetic field, and carrier concentration [20–24]. Currently, the critical exponents $z\nu$ for the SIT is rather controversial in different cuprate systems [8,9,13,14,18]. By carefully controlling the disorder levels, Yu *et al.* have divided the system to the clean and dirty limits, which dominates the detailed critical behaviors [18]. This argument still needs further verification by more experiments.

In this paper, we report the discovery of a universal relation between the doping content p and the normal-state resistance at a fixed temperature $R(T_f)$, $p = \alpha + \beta \ln[1/R(T_f)]$, in the gate voltage tuned ultra-thin Bi-2212. This relation works

*jiangda77@hotmail.com

†mugang@mail.sim.ac.cn

satisfactorily in the two samples of this work and the samples of two other groups [14,18], representing a quite good universality. Based on this relation, the doping content in the heavily underdoped region is calculated and the more precise phase diagram can be acquired. Further analysis reveals that the scattering probability $1/\tau$ could not be treated as a constant in the tuning process. Our data also indicates the drastic change in carrier effective mass m^* due to the superconductor-insulator transition. Moreover, finite size scaling analysis is adopted to investigate the temperature dependent resistance data and a superconductor-insulator quantum phase transition is revealed. The scaling exponent $z\nu$ is determined to be 2.86 and 1.50 for the samples with a high and low level of disorder, respectively. Our result verifies that disorder is indeed a key factor in determining the behavior of the SIT.

II. EXPERIMENTAL

The Bi-2212 single crystals were grown by the traveling-solvent floating zone method [25]. The mechanical exfoliation method was employed to fabricate the ultra-thin samples. The Bi-2212 ultra-thin flakes were exfoliated from the single crystal by Nitto tape and transferred onto the solid ion conductor (SIC) substrate [26,27]. The SIC substrate is Li^+ ion conducting glass ceramic (PrMat, $\text{Li}_2\text{O}-\text{Al}_2\text{O}_3-\text{SiO}_2-\text{P}_2\text{O}_5-\text{TiO}_2$). The fabricating process was carried out in an atmospheric environment. The SC properties of the ultra-thin samples can survive in air for dozens of minutes. Sample S-1 was exposed in air for seven minutes after the fabrication, while sample S-2 was exposed for four minutes. Typically the in-plane dimension of the fabricated samples can be as large as 300 μm . The morphology and thicknesses of films were measured by an atomic force microscope (AFM, Bruker Dimension Icon). As can be seen in the Supplementary Material (SM) (Fig. S1) [28], the thickness of the samples in the present study is two unit cells.

The electrical resistance was measured in the physical property measurement system (Quantum Design, PPMS) by a standard four-probe method. The silver paste was used to prepare the electrodes. The gate voltage was tuned at 260 K, where Li^+ ion mobility inside the glass is activated. The gate voltage is below 1 V and the duration time at the doping temperature for the voltage gate tuning varied from 10 to 30 minutes depending on the initial and final doping levels.

III. RESULTS

A. SIC-assisted gate voltage tuning on the superconductivity

We concentrate our study on two samples, S-1 and S-2, with different disorder levels tuned by the exposure time in air. As we have mentioned in the Experimental section, S-1 and S-2 were exposed to air for seven and four minutes, respectively, after they were mechanically exfoliated. Consequently S-1 has a relatively higher level of disorder compared with S-2. In addition, we found that the oxygen concentration in the ultra-thin sample can be increased in the process of exposing to air for several minutes [see Fig. S2(a) in SM], which introduces extra hole doping into the sample. In this sense, sample S-2 should be more underdoped than S-1. This tendency is consistent with the result reported by Yu *et al.* [18].

As shown in Figs. 1(a)–1(c), with the aid of SIC [see the inset of Fig. 1(a)], the temperature dependent resistance of S-1 can be tuned continuously by gate voltage from the original curve (labeled with A). With the increase of the duration time at 260 K under the positive gate voltage, where the ions in the SIC are mobile, the superconducting (SC) transition temperature is enhanced slightly (A \rightarrow B) and then decreased towards zero (B \rightarrow O), revealing the evolution from the slightly overdoped region via the optimal doped point to the underdoped region. Meanwhile, the magnitude of resistance in the normal state is increased monotonically and the insulating behavior emerges after the superconductivity vanishes. Resistance of S-2 shows roughly similar evolution to that observed in S-1, see Figs. 1(d) and 1(e). The only difference is the relatively lower T_c in sample S-2 as it is more underdoped.

Typically, electrostatic carrier accumulation, oxygen-vacancy injection, and Li^+ intercalation through the basal plane could be the most probable mechanisms for the doping effect in the SIC-assisted gating process. From the previous report with the similar SIC-assisted configuration [13], the density of Li^+ ions can reach a considerably high level in Bi-2212, suggesting that the Li^+ intercalation could be the dominant mechanism for the doping evolution in the present experiment.

Figure 1(f) describes the details for determining the SC critical transition temperature. After the normal state resistance R_n is fixed by the intersection of the two dashed extrapolated lines, three critical points $T_{c,90\%R_n}$, $T_{c,50\%R_n}$, and $T_{c,10\%R_n}$ can be obtained. Another criterion, the maximum of the differential dR/dT , is also adopted, which gives $T_{c,diff}$.

B. Determination of the doping content p

To demonstrate the evolution of these critical temperatures with doping content, we first estimated the doping level from the resistance value at a fixed temperature T_f ,

$$p_R = S/R(T_f). \quad (1)$$

This relation, assuming that the carrier scattering probability and effective mass are constants based on the Drude picture, was frequently used in the two-dimensional cuprate systems [8,9,13,18]. In Fig. 2(a), we show the result of S-1 with $T_f = 150$ K. The value of S is fixed as 178 so that the optimal point is located at $p_R = 0.16$. At this optimal point, $T_{c,90\%R_n}$ and $T_{c,50\%R_n}$ are as high as 95.6 K and 90.7 K, respectively. These data are compared with the generic relation [29]

$$T_c(p)/T_c(p_{opt}) = 1 - 82.6(p - p_{opt})^2, \quad (2)$$

where p_{opt} is the optimal doping level which is fixed as 0.16. Typically the applicability of this equation is only affected by the disorder at the position of Cu atoms [5]. Thus, Eq. (2) can be safely used in the system we are studying. As shown by the olive solid line in Fig. 2(a), this relation deviates from the experimental data obviously. The situation with $T_f = 200$ K (see Fig. S6 in the SM) is similar. Thus the simple hypothesis for the Drude model is not tenable in the present system. This problem has been noticed by other groups [12,14]. Actually, the magnitude of doping content p can be calculated from

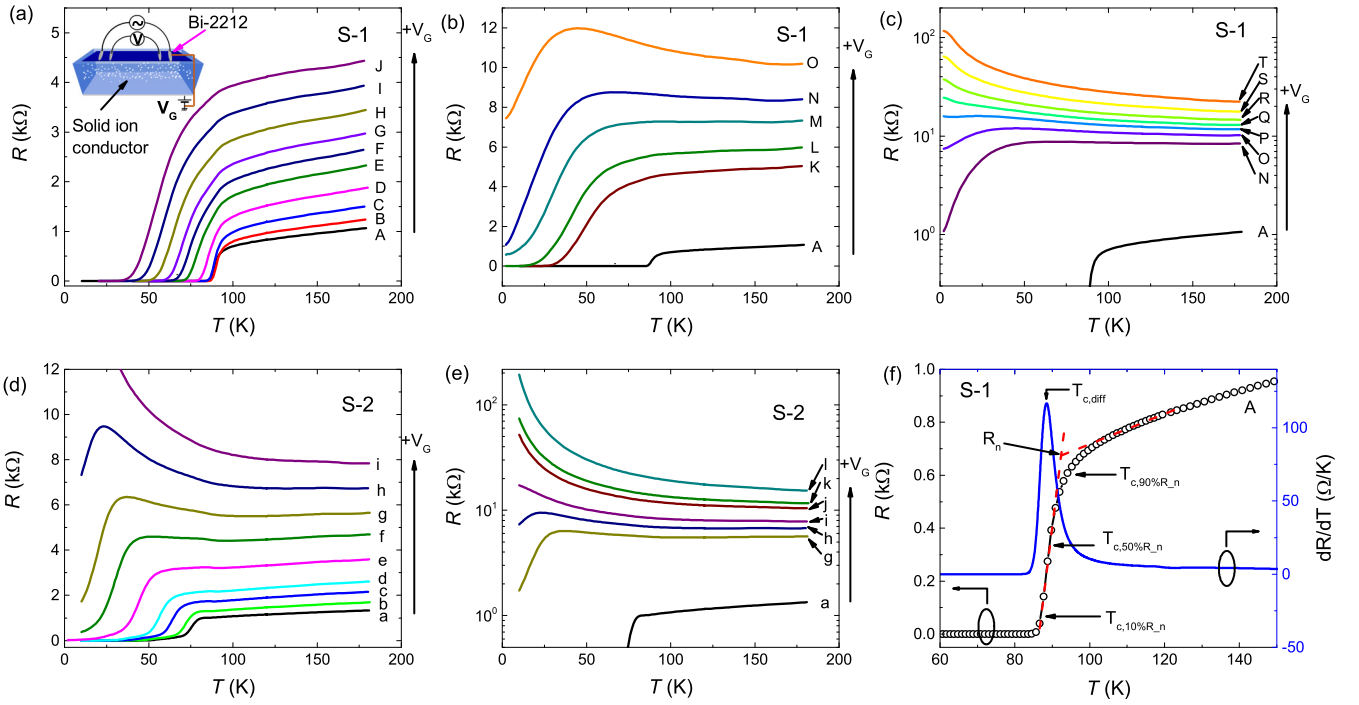


FIG. 1. Temperature dependence of the longitudinal resistance of the ultra-thin Bi-2212 samples S-1 (a)–(c) and S-2 (d) and (e). The inset of (a) shows a schematic view of the measurement setup. The arrowed lines indicate the directions in which the positive gate voltage increases. (f) Temperature-dependent resistance (black circles) and its derivative (blue curve) of the sample S-1 (the pristine state, A curve). Different methods for the determination of T_c (including $T_{c,10\%R_n}$, $T_{c,50\%R_n}$, $T_{c,90\%R_n}$, and $T_{c,diff}$), are illustrated.

Eq. (2) in the SC state because the values of $T_c(p)$ is available. The main problem is how to determine the doping levels in the non-SC state. Wang *et al.* utilized a linear dependence of T_c on $1/R(T_f)$ in the heavily underdoped region to estimate the doping content in the non-SC region [14]. However, such a linear tendency is absent in our data [see Fig. 2(a)] and

the data of Yu *et al.* [18]. Consequently, this approach is not universal and not conducive to be extended to other systems.

To conquer this problem, we calculated the p values in the SC state using Eq. (2) and examined the evolution of obtained p with $1/R(T_f)$ carefully. In the calculation, $T_{c,50\%R_n}$ is used, which will be abbreviated as T_c hereafter. As can be seen in

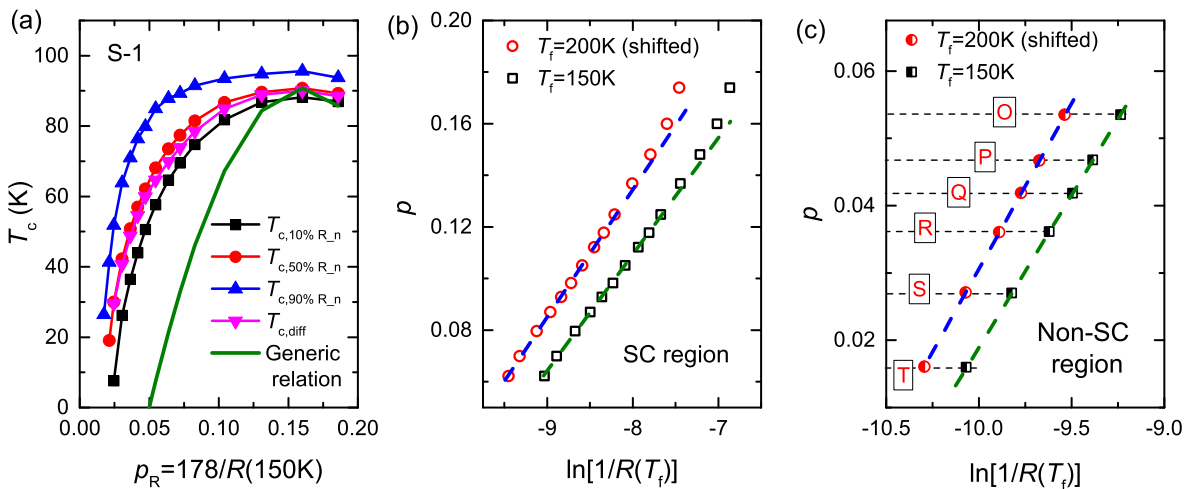


FIG. 2. (a) The SC critical temperatures determined using different methods as a function of $p_R = 178/R(150\text{K})$ for sample S-1. The olive solid line represents the generic relation discovered in the bulk samples [see Eq. (2) in the text]. (b) Doping levels in the SC region calculated using Eq. (2) as a function of $\ln[1/R(T_f)]$. The data with $T_f = 150\text{K}$ and 200K are shown together. The data of 200K are shifted to the left by 0.4 for clarity. The straight dashed lines are the results of linear fitting in the underdoped region $p < 0.13$. (c) Doping levels as a function of $\ln[1/R(T_f)]$ in the non-SC region. The data of 200K are shifted to the left by 0.3 for clarity. The straight dashed lines are the results of linear fitting. The capital letters correspond to different levels of the gate tuning as shown in Figs. 1(a) and 1(b).

TABLE I. Summary of the parameters in Eq. (3) and the calculated p in the non-SC region for S-1 at two temperatures 150 K and 200 K.

T_f	α	β	$p(O)$	$p(P)$	$p(Q)$	$p(R)$	$p(S)$	$p(T)$
150 K	0.470	0.0451	0.05353	0.04680	0.04186	0.03617	0.02703	0.01598
200 K	0.511	0.0495	0.05351	0.04673	0.04187	0.03612	0.02706	0.01603

Fig. S7 in the SM, $p - 1/R(T_f)$ curve reveals an obviously nonlinear tendency, especially in the region with $p \leq 0.10$. Nevertheless, as shown in Fig. 2(b), p displays a fine linear dependence with logarithm of $1/R(T_f)$ in the region $p \leq 0.13$. In this figure, the data at two different T_f (150 K and 200 K) are shown together, both of which reveal the very similar tendency. This behavior can be observed in a wide temperature range $100 \text{ K} \leq T_f \leq 250 \text{ K}$, which will be discussed in details in the next paragraph. The linear behavior can be described by a simple relation

$$p = \alpha + \beta \ln[1/R(T_f)], \quad (3)$$

where α and β are the fitting parameters. After obtaining the values of α and β by fitting the data in Fig. 2(b), the doping levels of the non-SC region can be calculated by substituting the $1/R(T_f)$ values into Eq. (3). The results for S-1 are summarized in Fig. 2(c) and Table I. It is worth noting that the calculated p values in the non-SC region using the $R(T_f)$ data with $T_f = 150 \text{ K}$ and 200 K are very close to each other. The deviation between them is below 1%. This confirms the reliability of the present analysis. Sample S-2 also reveals the similar tendency, which is shown in the SM [see Fig. S8(a)]. Moreover, the data from Yu's [18] and Wang's [14] groups are also analyzed with the same process, both of which obey the Eq. (3) we proposed above [see Figs. S8(b) and (c) in the SM]. Particularly in Yu's work, the doping level of the ultra-thin samples was tuned by controlling the oxygen content in an annealing process. Thus the relation revealed in Eq. (3) is quite universal in the ultra-thin Bi-2212 system, regardless of the tuning routes.

To acquire additional information about the parameters α and β , we checked the $p - \ln[1/R(T_f)]$ curves in a wide temperature range ($100 \text{ K} \leq T_f \leq 250 \text{ K}$) for S-1, see Fig. 3(a). The linear dependence of p on $\ln[1/R(T_f)]$ is observed in the whole temperature range in the underdoped side, indicating that the relation in Eq. (3) works quite well in a wide temperature range from 100 K to 250 K. By fitting these curves using Eq. (3), temperature dependent values of α and β can be obtained, which are shown in Fig. 3(b).

C. Electronic phase diagram

As the doping content p has been determined reliably, we can draw the electronic phase diagram for the gate voltage tuned system. Here we show the result of S-1 as an example. As can be seen in Fig. 4, the contour map of the resistance represents clearly the boundary between SC and normal states. The T_c data determined by $50\% R_n$ is also shown for reference. The roughly vertical contour line of $10 \text{ k}\Omega$ separates the metallic and insulating regions in the normal state (typically above 50 K in the heavily underdoped region). The white dashed line indicates the position of the SIT (see the next section), which resides very close to the edge of the SC dome.

D. Superconductor-insulator transition

From the $R-T$ curves in Figs. 1(c) and 1(e), a clear SIT induced by gate voltage is revealed for both S-1 and S-2. Here we replot the data as R versus p in the low temperature region below 25 K , see Figs. 5(a) and 5(c). All curves intersect at one critical point p_c (0.047 and 0.051 for S-1 and S-2, respectively). Such a doping (rather than temperature) controlled transition is a candidate for the quantum phase transition (QPT). The physical properties near the critical point of QPT is typically analyzed by finite-size scaling method, which states that resistance near the critical point can be described by the critical exponents (z, ν) and the distance from the critical point $|p - p_c|$ in the relationship [30,31]

$$R(p, T) = R_c F[(p - p_c)T^{-1/z\nu}], \quad (4)$$

where p_c is the critical point, ν is the correlation-length exponent, z is the dynamical-scaling exponent, and F is an arbitrary function with $F(0) = 1$. The value of $z\nu$ is tuned to achieve a fine scaling behavior.

As shown in Figs. 5(b) and 5(d), all the experimental data collapse into a single curve, indicating the occurrence of a superconductor-insulator QPT induced by doping. From this scaling, the critical exponents $z\nu = 2.86$ and 1.50 are obtained for samples S-1 and S-2, respectively. The critical resistances per square (R_c) are about 32 and $22 \text{ k}\Omega$ for S-1 and S-2, which are obviously larger than the quantum resistance $R_Q = h/(2e)^2 = 6.45 \text{ k}\Omega$. We note that the values of R_c obtained here have a relatively large uncertainty due to the difficulty in precisely determining the dimension of the electrodes.

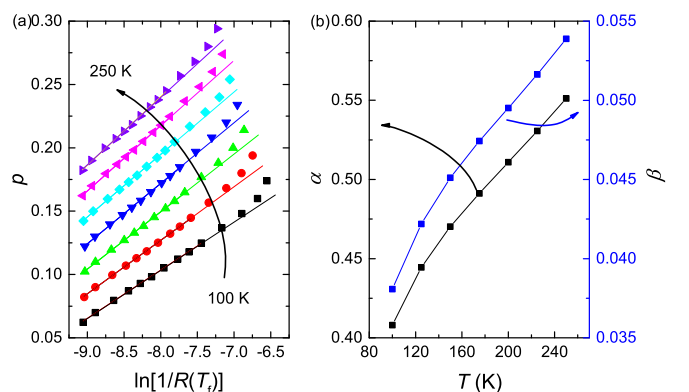


FIG. 3. (a) The doping levels calculated using Eq. (2) (see text) as a function of $\ln[1/R(T_f)]$ in a wide temperature range $100 \text{ K} \leq T_f \leq 250 \text{ K}$ for sample S-1. The temperature interval is 25 K . The data at each fixed temperature has been shifted upwards by 0.02 for clarity. The straight dashed lines are the results of linear fitting in the underdoped region $p < 0.13$. (b) Fitting parameters α and β as a function of T .

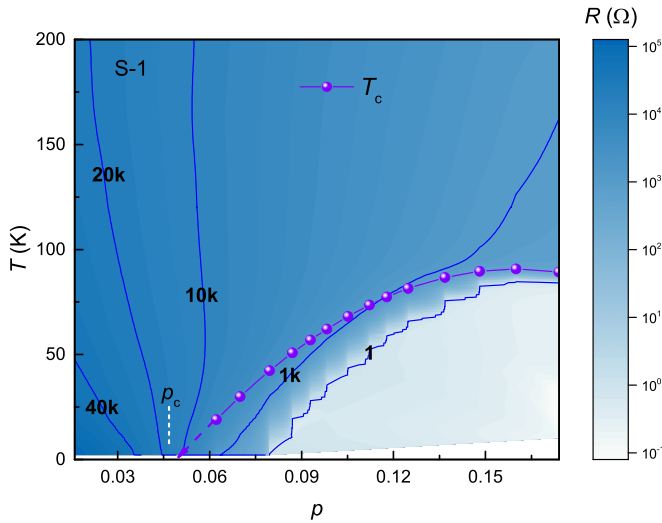


FIG. 4. Phase diagram for the gate voltage tuned ultra-thin Bi-2212. The contour map represents the magnitude of resistance. The T_c data using the criterion of 50% R_n is also shown. The solid blue lines are the contour lines of selected values of resistance (the unit is Ω). The white dashed line indicates the position of the SIT.

In order to illustrate the influence of precise determination of the doping contents on the quantum phase transition, we show the phase transition analysis based on the doping contents determined from Eq. (1) in the SM [28], see Fig. S9. One can see that the route for the determination of p can affect both the position of critical point and the critical exponents.

IV. DISCUSSION

The simple relation $p_R = S/R(T_f)$ is applicable to ultrathin $\text{YBa}_2\text{Cu}_3\text{O}_{7-x}$ films and 40 nm thick Bi-2212 flakes [9,13].

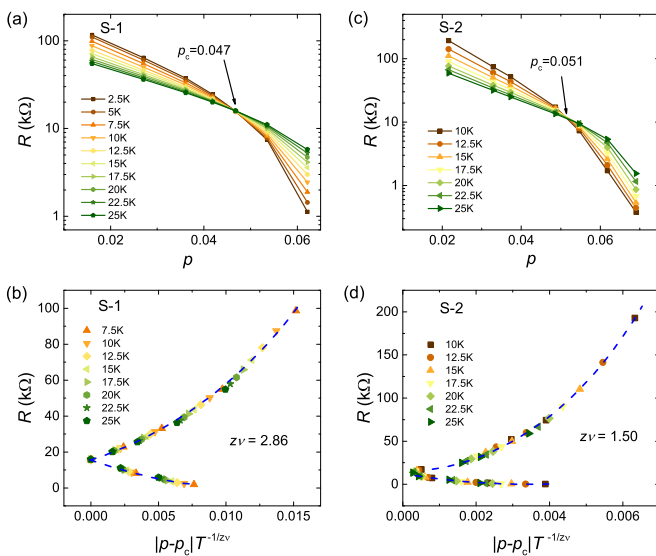


FIG. 5. (a, c) Doping dependence of resistance in the temperature region below 25 K of samples S-1 and S-2 respectively. (b, d) Resistance of samples S-1 and S-2 respectively as a function of scaling variable $|p - p_c|T^{-1/z\nu}$. The blue dashed lines are visual guides.

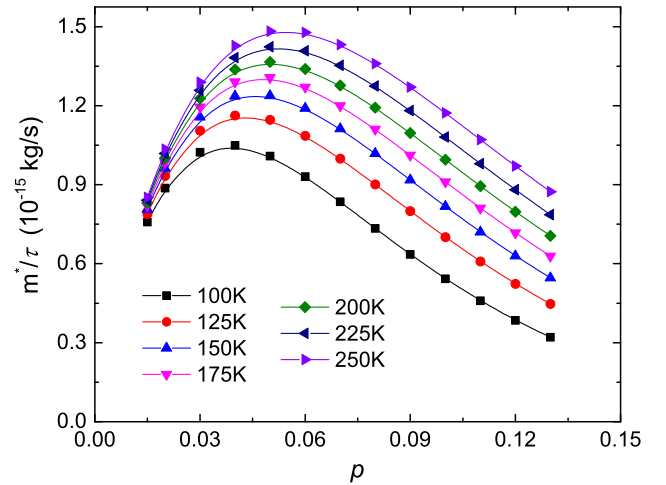


FIG. 6. The evolution of m^*/τ as a function of the doping content p calculated using Eq. (5).

It fails in the Bi-2212 system with the thickness less than or equal to two unit cells [12,14]. These facts indicate that, at least for Bi-2212 system, thickness may be an important factor. For the YBCO film, although the superconducting layer is only one to two unit cells, an insulating layer with the thickness of five to six unit cells are covered on it. The possible influence of this insulating layer on the low-dimensional system is still unknown.

In order to have a comprehensive understanding of the unique feature in the ultra-thin Bi-2212 system, we consider the influences of the relaxation time τ and effective mass m^* on the electrical transport. The conductivity can be expressed as

$$\sigma = nq^2\tau/m^*, \quad (5)$$

where q is the elementary charge and $n = p \times x$ is the carrier concentration. Here $x = 8.9 \times 10^{27} \text{ m}^{-3}$ is the concentration of Cu atoms in Bi-2212. With the combination with Eq. (3), we can derive the following relation,

$$\frac{m^*}{\tau} = Ape^{-p/\beta}, \quad (6)$$

where $A = xq^2e^{\alpha/\beta}S/l$. S and l are the cross-sectional area and distance between the voltage leads of the measured sample, respectively. By substituting the values of these parameters, the value of A is obtained to be about $7.5 \times 10^{-14} \text{ kg/s}$. In order to have an intuitive impression, we represent this relation in Fig. 6. The data are shown in a limited doping range below 0.13, where Eq. (3) holds. Although the accuracy of this set of data may be limited by the somewhat inaccurate determination of the sample dimension, we can still obtain important information from the evolution trend of m^*/τ with p .

In the high- T_c superconducting system with strong correlation, the transition to insulating state is closely related to the enhancement of the effective mass [31]. Thus, m^* will increase significantly near the SIT point. While in the doping region far away from the phase transition point, m^* will change less violently, which can be roughly treated as a constant. In this case, Eq. (6) actually reflects the relation between

TABLE II. Summary of the critical exponent $z\nu$ in the ultra-thin cuprate systems.

Sample ^a	Thickness	$z\nu$	Ref.
LSCO	1 unit cell	1.5	[8]
YBCO	1-2 unit cells ^b	2.2	[9]
PCCO	1 unit cell	2.4	[11]
Bi-2212	40 nm	1.5	[13]
Bi-2212 ^c	1 unit cell	1.57	[14]
Bi-2212	a half unit cell	1.53, 2.45, 2.35 ^d	[18]
Bi-2212	2 unit cells	1.50, 2.86 ^e	This work

^aLSCO, YBCO, PCCO, and Bi-2212 are the abbreviations of $\text{La}_{2-x}\text{Sr}_x\text{CuO}_4$, $\text{YBa}_2\text{Cu}_3\text{O}_{7-x}$, $\text{Pr}_{2-x}\text{Ce}_x\text{CuO}_4$, and $\text{Bi}_2\text{Sr}_2\text{CaCu}_2\text{O}_{8+x}$, respectively.

^bThe first five to six unit cells are insulating. Thus the film with the thickness of seven unit cells has a superconducting layer that is actually only one to two unit cells thick.

^cSr is partially doped with Bi ($x = 0.1$).

^dThe disorder was tuned by annealing the samples in different atmospheres.

^eThe disorder was tuned by changing the duration time in air after the samples are exfoliated.

scattering probability $1/\tau$ and the doping content p . At a fixed temperature, $1/\tau$ increases monotonically with the decrease of p down to about 0.06. This trend undoubtedly shows that the SIC-assisted gate voltage tuning not only changes the carrier concentration, but also has a significant impact on the scattering probability of the carriers. At the same time, this fact also explains why the previous simple equation, $p_R = S/R(T_f)$, is no longer applicable in this system. It should be pointed out that a large part of the increase of $1/\tau$ should come from the enhancement of disorder in the tuning process. The influences of ion-gating induced disorder has been reported in transition metal disulfides [32,33]. Such disorders are not located at the position of Cu atoms, so it has no significant effect on the values of T_c and the T_c - p phase diagram.

At around $p=0.05$, where the superconductor-insulator transition occurs (see Fig. 5), the monotonic increasing trend of m^*/τ with the decrease of p is reversed. Actually, this reflects the change of carrier effective mass m^* caused by the drastic change of the band structure accompanying the SIT. As we have mentioned, the effective mass enhancement is a typical feature for strongly correlated systems near the phase transition point [31]. The consistency of the location of these two events, SIT and the reversal in the m^*/τ - p curves, verifies the reliability of our analysis.

On the other hand, it has been noticed that the critical exponent $z\nu$ for the SIT is quite scattering in the ultra-thin cuprate systems [8,9,11,13,14,18]. In the epitaxial films of $\text{La}_{2-x}\text{Sr}_x\text{CuO}_4$ with the thickness of one unit cell [8], $z\nu$ was found to be 1.5. While in the ultrathin $\text{YBa}_2\text{Cu}_3\text{O}_{7-x}$ films [9], $z\nu = 2.2$. Even in the same Bi-2212 system, a universal result is still not achieved [13,14,18]. Table II summarizes the typical reports in recent years. In general, $z\nu = 4/3$ is a hallmark for the classical percolation model [21,34], while $z\nu = 7/3$ and $2/3$ are predicted by the quantum percolation model [35] and 3D XY model [36], respectively. As has been pointed out by Yu *et al.*, these data focus on

two values, $3/2$ and $7/3$, which were attributed to the different degrees of the disorder [18]. For sample S-2, the $z\nu$ value (1.50) is consistent with this classification. However, $z\nu = 2.86$ in S-1 is clearly larger than $7/3$. Considering the relatively longer duration time in air for S-1, which may introduce more disorder in the sample, it seems that the levels of disorder have a direct influence on the critical exponent, consistent with the argument of Yu *et al.*, [18] qualitatively.

In the ultrathin Bi-2212 system, an obvious feature brought about by the increase of disorder is that, the rising trend of resistance in the insulating state with the decrease of temperature will be suppressed [18]. In order to provide more convincing information about the differences in disorder between the two samples, we compared their resistance behavior in the insulating state, as shown in Fig. S10. Obviously, compared with sample S-2, the rising trend of resistance of S-1 is significantly weakened. Thus, there is relatively more disorder in sample S-1, which is consistent with the longer exposure time of sample S-1 in air.

Finally, we need to point out that, considering the fact that the SIC-assisted gate tuning process will also affect the disorder of the samples, the SIT observed here is not simply induced by the evolution of doping contents, but by both the doping and disorder.

V. CONCLUSION

In summary, we tuned the electronic state of the ultra-thin Bi-2212 superconductors using gate voltage with the aid of SIC. A universal relation, $p = \alpha + \beta \ln[1/R(T_f)]$, was discovered in the underdoped region of this system. Further analysis reveals that two factors play important roles in determining the transport behavior of ultra-thin Bi-2212: (1) the evolution of carrier scattering probability with the gate voltage tuning and (2) the change in effective mass due to the superconductor-insulator transition. Based on the present finding, a solid determination for the doping content in the heavily underdoped non-SC region was made and the precise phase diagram was obtained. In addition, the doping induced superconductor-insulator QPT was found in two samples with the critical exponent $z\nu = 2.86$ and 1.50 respectively. A detailed analysis shows that the level of disorder may be an important factor affecting the critical exponent of the SITs.

ACKNOWLEDGMENTS

We thank Prof. Y. B. Zhang for the fruitful discussion. This work was supported by the National Natural Science Foundation of China (Grants No. 11204338 and No. 51925208), the Strategic Priority Research Program of Chinese Academy of Sciences (Grant No. XDB30000000), and the Youth Innovation Promotion Association of the Chinese Academy of Sciences (Grant No. 2015187). The work was also supported by talents' plan launch funding of Zhejiang University of Technology (Grant No. 202241637029), Research funding of Institute for Frontiers and Interdisciplinary Sciences of Zhejiang University of Technology, and DOE Office of Science by Brookhaven National Laboratory in U.S. (Grant No. DE-SC0012704).

- [1] K. Karpińska, A. Malinowski, M. Z. Cieplak, S. Guha, S. Gershman, G. Kotliar, T. Skośkiewicz, W. Plesiewicz, M. Berkowski, and P. Lindendorf, *Phys. Rev. Lett.* **77**, 3033 (1996).
- [2] G. S. Boebinger, Y. Ando, A. Passner, T. Kimura, M. Okuya, J. Shimoyama, K. Kishio, K. Tamasaku, N. Ichikawa, and S. Uchida, *Phys. Rev. Lett.* **77**, 5417 (1996).
- [3] B. Beschoten, S. Sadewasser, G. Güntherodt, and C. Quitmann, *Phys. Rev. Lett.* **77**, 1837 (1996).
- [4] C. Quitmann, D. Andrich, C. Jarchow, M. Fleuster, B. Beschoten, G. Güntherodt, V. V. Moshchalkov, G. Mante, and R. Manzke, *Phys. Rev. B* **46**, 11813 (1992).
- [5] S. Naqib, J. Cooper, J. Tallon, and C. Panagopoulos, *Physica C: Superconductivity* **387**, 365 (2003).
- [6] Y. Ando, S. Komiya, K. Segawa, S. Ono, and Y. Kurita, *Phys. Rev. Lett.* **93**, 267001 (2004).
- [7] N. Barišić, M. K. Chan, Y. Li, G. Yu, X. Zhao, M. Dressel, A. Smontara, and M. Greven, *Proc. Natl. Acad. Sci.* **110**, 12235 (2013).
- [8] A. T. Bollinger, G. Dubuis, J. Yoon, D. Pavuna, J. Misewich, and I. Božović, *Nature (London)* **472**, 458 (2011).
- [9] X. Leng, J. Garcia-Barriocanal, S. Bose, Y. Lee, and A. M. Goldman, *Phys. Rev. Lett.* **107**, 027001 (2011).
- [10] J. Garcia-Barriocanal, A. Kobrinskii, X. Leng, J. Kinney, B. Yang, S. Snyder, and A. M. Goldman, *Phys. Rev. B* **87**, 024509 (2013).
- [11] S. W. Zeng, Z. Huang, W. M. Lv, N. N. Bao, K. Gopinadhan, L. K. Jian, T. S. Herrg, Z. Q. Liu, Y. L. Zhao, C. J. Li *et al.*, *Phys. Rev. B* **92**, 020503 (2015).
- [12] E. Sterpetti, J. Biscaras, A. Erb, and A. Shukla, *Nat. Commun.* **8**, 2060 (2017).
- [13] M. Liao, Y. Zhu, J. Zhang, R. Zhong, J. Schneeloch, G. Gu, K. Jiang, D. Zhang, X. Ma, and Q. K. Xue, *Nano Lett.* **18**, 5660 (2018).
- [14] F. Wang, J. Biscaras, A. Erb, and A. Shukla, *Nat. Commun.* **12**, 2926 (2021).
- [15] J. M. Lu, O. Zheliuk, I. Leermakers, N. F. Q. Yuan, U. Zeitler, K. T. Law, and J. T. Ye, *Science* **350**, 1353 (2015).
- [16] Y. Saito, Y. Kasahara, J. Ye, Y. Iwasa, and T. Nojima, *Science* **350**, 409 (2015).
- [17] Y. Saito, Y. Nakamura, M. S. Bahramy, Y. Kohama, J. Ye, Y. Kasahara, Y. Nakagawa, M. Onga, M. Tokunaga, T. Nojima *et al.*, *Nat. Phys.* **12**, 144 (2016).
- [18] Y. Yu, L. Ma, P. Cai, R. Zhong, C. Ye, J. Shen, G. Gu, X. H. Chen, and Y. Zhang, *Nature (London)* **575**, 156 (2019).
- [19] V. F. Gantmakher and V. T. Dolgoplov, *Phys. Usp.* **53**, 1 (2010).
- [20] N. Marković, C. Christiansen, and A. M. Goldman, *Phys. Rev. Lett.* **81**, 5217 (1998).
- [21] A. Yazdani and A. Kapitulnik, *Phys. Rev. Lett.* **74**, 3037 (1995).
- [22] J. Biscaras, N. Bergeal, S. Hurand, C. Feuillet-Palma, A. Rastogi, R. C. Budhani, M. Grilli, S. Caprara, and J. Lesueur, *Nat. Mater.* **12**, 542 (2013).
- [23] Y. Sun, H. Xiao, M. Zhang, Z. Xue, Y. Mei, X. Xie, T. Hu, Z. Di, and X. Wang, *Nat. Commun.* **9**, 2159 (2018).
- [24] R. Schneider, A. G. Zaitsev, D. Fuchs, and H. v. Löhneysen, *Phys. Rev. Lett.* **108**, 257003 (2012).
- [25] J. Wen, Z. Xu, G. Xu, M. Hücker, J. Tranquada, and G. Gu, *J. Cryst. Growth* **310**, 1401 (2008).
- [26] K. S. Novoselov, A. K. Geim, S. V. Morozov, D. Jiang, Y. Zhang, S. V. Dubonos, I. V. Grigorieva, and A. A. Firsov, *Science* **306**, 666 (2004).
- [27] D. Jiang, T. Hu, L. You, Q. Li, A. Li, H. Wang, G. Mu, Z. Chen, H. Zhang, G. Yu *et al.*, *Nat. Commun.* **5**, 5708 (2014).
- [28] See Supplemental Material at <http://link.aps.org/supplemental/10.1103/PhysRevB.106.104509> for details of the preparation and characterization of ultrathin Bi-2212 flakes; the effects of atmospheres on resistance samples; the universality of the relation between p and $R(T_f)$ [Eq. (3)]; the finite-size scaling of SIT using p_R as the doping content; and a comparison of the insulating behaviors in S-1 and S-2.
- [29] M. Presland, J. Tallon, R. Buckley, R. Liu, and N. Flower, *Physica C: Superconductivity* **176**, 95 (1991).
- [30] S. L. Sondhi, S. M. Girvin, J. P. Carini, and D. Shahar, *Rev. Mod. Phys.* **69**, 315 (1997).
- [31] M. Imada, A. Fujimori, and Y. Tokura, *Rev. Mod. Phys.* **70**, 1039 (1998).
- [32] D. Ovchinnikov, F. Gargiulo, A. Allain, D. J. Pasquier, D. Dumcenco, C. H. Ho, O. V. Yazyev, and A. Kis, *Nat. Commun.* **7**, 12391 (2016).
- [33] E. Piatti, Q. Chen, and J. Ye, *Appl. Phys. Lett.* **111**, 013106 (2017).
- [34] Y. Ma, G. Mu, T. Hu, Z. Zhu, Z. Li, W. Li, Q. Ji, X. Zhang, L. Wang, and X. Xie, *Sci. China: Phys., Mech. Astron.* **61**, 127408 (2018).
- [35] D.-H. Lee, Z. Wang, and S. Kivelson, *Phys. Rev. Lett.* **70**, 4130 (1993).
- [36] Y.-H. Li and S. Teitel, *Phys. Rev. B* **40**, 9122 (1989).